



# The administration of *Escherichia coli* Nissle 1917 ameliorates irinotecan-induced intestinal barrier dysfunction and gut microbial dysbiosis in mice

Yurong Wang<sup>1</sup>, Lie Sun<sup>1</sup>, Shanwen Chen, Shihao Guo, Taohua Yue, Qisheng Hou, Mei Feng, Hao Xu, Yucun Liu, Pengyuan Wang, Yisheng Pan\*

Division of General Surgery, Peking University First Hospital, Peking University, 8 Xi ShiKu Street, Beijing 100034, People's Republic of China

## ARTICLE INFO

### Keywords:

Irinotecan  
EcN  
Chemotherapy  
Tight junction  
Claudin-1  
Gut microbiota

## ABSTRACT

**Aims:** The present study investigated the effect of *Escherichia coli* Nissle 1917 (EcN) on irinotecan-induced intestinal barrier dysfunction and gut microbial dysbiosis in a mouse model and in the human colonic cells lines Caco-2.

**Materials and methods:** Male BALB/c mice received irinotecan intraperitoneal injection with or without EcN administration intragastrically. Body weight, diarrhea severity, intestinal permeability and histopathological analysis of ileum epithelia of mice from different groups were assessed. The expression and localization of tight junction proteins were examined using western blot and immunofluorescence. Gut microbiota structure and diversity were measured with 16 S rRNA sequencing. Caco-2 monolayers were incubated with EcN culture supernatant (EcN<sup>sup</sup>) or SN-38 and the monolayer barrier function was assessed by transepithelial electrical resistance (TER) and FITC-dextran 4000 Da (FD-4) flux.

**Key findings:** Pretreatment with EcN significantly attenuated irinotecan-induced weight loss and diarrhea in mice. In addition, EcN inhibited the increased intestinal permeability and decreased Claudin-1 expression in irinotecan-treated mice. Furthermore, irinotecan treatment decreased the diversity of gut microbiota and increased the relative abundance of Proteobacteria compared to control group. EcN administration ameliorated the gut microbiota dysbiosis. In Caco-2 monolayers, EcN<sup>sup</sup> ameliorated the decreased TER and increased FD-4 flux elicited by SN-38. Moreover, EcN<sup>sup</sup> attenuated SN-38-induced altered localization and distribution of Claudin-1 in Caco-2 monolayers.

**Significance:** Our results indicated that the administration of EcN protected against irinotecan-induced intestinal injury by regulating intestinal barrier function and gut microbiota.

## 1. Introduction

Irinotecan, a topoisomerase I inhibitor, is widely used in the treatment of advanced colorectal cancer. However, almost 50–80% of patients receiving irinotecan develop intestinal mucositis with diarrhea as the most common manifestation, which severely compromises the living quality of patients [1]. The intestinal damage induced by irinotecan is featured by increased apoptosis in crypts and loss of villi [2]. Irinotecan is metabolized mainly by hepatic carboxylesterases to form an active metabolite, SN-38, which is subsequently metabolized by uridine diphosphate-glucuronosyltransferase 1A1 (UGT1A1) into

SN-38-glucuronide (SN-38G) [3]. After being secreted into the intestine, SN-38G is reactivated into SN-38 by  $\beta$ -glucuronidase-positive Enterobacteriaceae. It is believed that SN-38 is involved in the development of irinotecan-induced mucositis by damaging intestinal mucosal epithelial cells [4].

Tight junctions localized in the apical-lateral margin of adjacent enterocytes play a vital role in maintaining intact intestinal barrier function [5]. Tight junctions consist of transmembrane proteins (Occludin and Claudins) and peripheral membrane proteins (ZO). ZO proteins (ZO-1, ZO-2, and ZO-3) are cytosolic scaffolds that anchor peripherally located transmembrane proteins to the actin cytoskeleton

**Abbreviations:** EcN, *Escherichia coli* Nissle 1917; EcN<sup>sup</sup>, *Escherichia coli* Nissle 1917 culture supernatant; FD-4, FITC-dextran 4000 Da; TER, transepithelial electrical resistance

\* Corresponding author.

E-mail address: [yisheng.pan@pkufh.com](mailto:yisheng.pan@pkufh.com) (Y. Pan).

<sup>1</sup> Contributed equally.

<https://doi.org/10.1016/j.lfs.2019.06.004>

Received 29 March 2019; Received in revised form 28 May 2019; Accepted 2 June 2019

Available online 04 June 2019

0024-3205/ © 2019 Elsevier Inc. All rights reserved.

and form the complete tight junction complex [6]. Alteration of tight junction contributed to intestinal barrier injury under pathological conditions, such as inflammatory bowel diseases [7] and intestinal infections [8]. In addition, a series of evidence suggested that the intestinal barrier injury caused by chemotherapeutic reagents is closely related to the disruption of tight junctions. Irinotecan significantly decreased Claudin-1 and Occludin expression in rats [9]. Besides, methotrexate treatment increased the intestinal permeability in rats, which is partially related to the reduction of Claudin-1 and Occludin expression [8].

Gut microbiota plays a vital role in maintaining the homeostasis of gastrointestinal tract. Natural intestinal microbiota interacts with the mucosal epithelium and performs diverse physiological functions such as regulation of immune and inflammatory response, modulation of integrity of the gut barrier and maintenance of substance metabolism [10]. Alteration of microbiota is associated with multiple diseases, such as gastrointestinal diseases [11] and metabolic diseases [12]. In addition, chemotherapy significantly induced the modification of gut microbiota. For instance, irinotecan increased the relative abundance of Fusobacteria and Proteobacteria in Sprague-Dawley rats [13]. Gut microbial dysbiosis is believed to be involved in the pathogenesis of intestinal damage induced by multiple factors [14]. Thus, balancing intestinal microbial homeostasis may be an alternative method to improve intestinal status.

Probiotics are defined as “Live microorganisms, which, when consumed in adequate amounts, confer a health benefit on the host” [15]. Recently, probiotics have been used to alleviate intestinal pathological state induced by chemotherapy. For example, *Saccharomyces cerevisiae* UFMG A-905 (Sc-905) prevented weight loss and intestinal lesions as well as maintained integrity of the mucosal barrier in irinotecan-treated mice [2]. *Escherichia coli* Nissle 1917 (EcN), a Gram-negative probiotic, has been widely studied for its therapeutic potential against a plethora of intestinal disorders, particularly in maintaining remission of ulcerative colitis [16]. The anti-inflammatory effect of EcN has been sufficiently illustrated [17]. In addition, EcN reinforces the intestinal epithelial barrier through upregulating tight junction proteins and increasing the expression of antimicrobial factors such as  $\beta$ -defensin-2 [5,18–20]. Furthermore, EcN was able to attenuate the DSS-induced gut microbial dysbiosis in mice, featured by an increase in bacterial diversity [21].

However, it still remains unclear whether EcN exerts protective effect against irinotecan-induced intestinal barrier dysfunction and gut microbial dysbiosis. Thus, we investigated the effect of EcN on the status of tight junction proteins and intestinal microbiota in mice receiving irinotecan. Besides, we further investigated the effect of EcN culture supernatant on epithelial barrier function in Caco-2 monolayers incubated with SN-38.

## 2. Materials and methods

### 2.1. Reagents and probiotics

*Escherichia coli* Nissle 1917 was purchased from Ardeypharm (Herdecke, Germany), irinotecan and SN-38 were obtained from MedChem Express (Princeton, USA), FITC-Dextran (4000 Da) was provided by Sigma-Aldrich (USA). The primary antibodies were purchased from the following companies: ZO-1 (Invitrogen, USA); Occludin (Invitrogen, USA); Claudin-1 (Invitrogen, USA); GAPDH (CST, USA). Species-specific secondary antibodies were obtained as follows: anti-rabbit and anti-mouse antibodies (CST, USA); Alexa 488-conjugated goat anti-rabbit antibody and Alexa 555-conjugated goat anti-mouse antibody (Invitrogen, USA).

### 2.2. Animals and experimental design

This study was conducted following the guidelines of the China

Laboratory Animal Management Committee and has been approved by the Animal Experimentation Ethics Committee of Peking University First Hospital. Male BALB/c mice (6–8 weeks old) obtained from Vital River Inc. (Beijing, China) were raised under a 12 h light/dark cycle at room temperature ( $23 \pm 2^\circ\text{C}$ ) with access to food and water ad libitum.

After one week of acclimatization, 32 mice were randomly divided into 4 groups: control group; irinotecan group; EcN + irinotecan group; heat-inactivated EcN + irinotecan group. The EcN + irinotecan group and heat-inactivated EcN + irinotecan group were daily treated with viable EcN or heat-inactivated EcN (carried out at  $95^\circ\text{C}$  for 15 min) gavage respectively at the concentration of  $1 \times 10^8$  CFU for 13 consecutive days, while the control and irinotecan groups received 200  $\mu\text{L}$  PBS. From day 10, irinotecan (150 mg/kg) was intraperitoneally injected in irinotecan group, EcN + irinotecan group and heat-inactivated EcN + irinotecan group once daily for 3 days. All the mice were sacrificed via carbon dioxide overdose at day 14.

Body weight and diarrhea severity of mice were recorded daily. Diarrhea severity was scored as described previously [22]: 0, normal (normal stool or absent); 1, slight (slightly wet and soft stool); 2, moderate (wet, unformed stool with perianal staining of the coat); and 3, severe (watery stool with perianal staining of the coat).

### 2.3. Measurement of intestinal barrier function

The intestinal permeability was measured as described previously [23]. Briefly, after 4 h of starvation, mice received gavage with FITC-dextran 4000 Da (FD-4) solution (600 mg/kg). Then, mice were sacrificed 4 h later, and blood was collected by cardiac puncture and then separated by centrifugation. Plasm levels of fluorescence intensity were measured using Synergy H2 microplate reader (Biotek Instruments, USA) (excitation, 490 nm; emission, 520 nm).

### 2.4. Histopathological analysis

Distal ileum was collected and fixed in 10% buffered formalin, dehydrated and embedded in paraffin as described previously [24]. Sections (4  $\mu\text{m}$ ) were obtained and stained with hematoxylin and eosin (H&E). Images were obtained using a Zeiss Image light microscope. The height of the intestinal villi and the depth of crypts were measured using ImageJ 1.8 software (NIH–National Institute of Health, Bethesda, MD, USA) for the villus/crypt ratio. 5 villi and crypts were measured per slice. Mucosal damage was also assessed as described by Macpherson & Pfeiffer with little modification [25] and was graded as follows: Score 0, normal histological findings; Score 1, mucosa: villus blunting, loss of crypt architecture, sparse inflammatory cell infiltration, vacuolization and edema. Muscle layer: normal. Score 2, mucosa: villus blunting with fattened and vacuolated cells, crypt necrosis, intense inflammatory cell infiltration, vacuolization and edema. Muscle layer: normal. Score 3, mucosa: villus blunting with fattened and vacuolated cells, crypt necrosis, intense inflammatory cell infiltration, vacuolization and edema. Muscle layer: edema, vacuolization and neutrophilic infiltration.

### 2.5. Western blot analysis

Ileum tissue was homogenized in RIPA lysis buffer supplemented with a cocktail of protease and phosphatase inhibitors, as previously described [26]. Similarly, the total protein of the Caco-2 cells was extracted as described previously [27]. The supernatant was collected after centrifugation, and protein concentration was determined by BCA Protein Assay Kit according to the manufacturer's instructions. Samples containing equal amounts of total protein were separated on a 4% to 12% gradient polyacrylamide gel and transferred onto PVDF membrane. The membranes were blocked with 5% (w/v) bovine serum albumin (BSA) solution 1 h at room temperature and incubated with

different primary antibodies against ZO-1, Occludin, Claudin-1, GAPDH overnight at 4 °C. Subsequently, the membrane was incubated with secondary antibodies at room temperature for 1 h. Bands were developed with electrochemiluminescence (ECL) detection reagents (Merck Millipore, USA).

## 2.6. Immunofluorescence

The immunofluorescence of ileum tissue was performed as described previously [28]. Briefly, sections (4 µm) were routinely deparaffinization and rehydrated. After heat-mediated antigen retrieval using 0.01 mol/L sodium citrate buffer (pH 6.0), slides were blocked by 0.1 mol/L PBS containing 10% normal goat serum. Subsequently, the slides were incubated with anti-ZO-1, anti-Occludin, anti-Claudin-1 primary antibodies overnight at 4 °C, followed by Alexa 488-conjugated goat anti-rabbit antibody and Alexa 555-conjugated goat anti-mouse antibody respectively for 1 h. The slides were stained with DAPI (4',6-diamidino-2-phenylindole). Immunofluorescence images were collected by Fluoview 1000 confocal microscope (Olympus, Japan) at 60× magnification.

Similarly, the immunofluorescence of Caco-2 monolayers was performed as previously demonstrated [29]. The Caco-2 monolayers were fixed in methanol at -20 °C overnight, followed by acetone at -20 °C for 1 min. After blocked with 1% bovine serum albumin (BSA) for 1 h at room temperature, the Caco-2 monolayers were then incubated with primary and secondary antibodies demonstrated above. Immunofluorescence images were collected by Fluoview 1000 confocal microscope (Olympus, Japan).

## 2.7. 16S rRNA gene sequence analysis

16S rRNA sequencing was performed as demonstrated previously [30]. Briefly, gut bacterial DNA from cecum contents of mice was extracted using commercial DNA Stool Mini extraction kit (Qiagen GmbH, Hilden, Germany), following the manufacturer's instructions. The V4 region of 16S rRNA gene of gut microbiota was amplified using forward primer 515 F (5'-GTGCCAGCMGCCGCGTAA-3') and reverse primer 806 R (5'-GGACTACHVGGGTWTCTAAT-3'). Samples were barcoded and pooled to build the sequencing library. The paired-end 2 × 250bp reads were generated with Illumina MiSeq platform (Illumina, San Diego, CA) and merged using FLASH, assigned to samples based on their unique barcodes. The high-quality clean tags were achieved under specific filtering conditions and then clustered to OTU (Operational Taxonomic Unit) by USEARCH with a 97% threshold of pairwise identity. The OTU unique representative sequences were obtained and taxonomically classified using the Greengenes database by Ribosomal Database Project (RDP) Classifier. The Alpha diversity was analyzed by Mothur, and the Beta diversity was analyzed using QIIME.

## 2.8. Cell culture

The human colonic cells lines Caco-2 were purchased from American Type Culture Collection and maintained in DMEM High Glucose supplemented with 10% FBS, 50 U/mL penicillin, 50 U/mL streptomycin and 25 mmol/L HEPES under 5% CO<sub>2</sub> at 37 °C. Only Caco-2 cell passages of 26–34 were used in this study.

## 2.9. Preparation of EcN culture supernatant

EcN culture supernatant (EcN<sup>sup</sup>) was used for this study. The preparation of EcN<sup>sup</sup> was described previously [5]. Briefly, EcN was grown in Luria-Bertani Broth and was resuspended with DMEM after centrifugated. After EcN was grown to an OD<sub>600</sub> of 1, the supernatant was collected by centrifugation (8000 × g, 15 min, 4 °C). Subsequently, the supernatant was filtrated with 0.22 µm-pore-size filter (Millipore) and then concentrated using Centricon Plus-20 centrifugal filters

(Millipore) with a molecular weight cutoff MWCO of 100kDa.

## 2.10. Transepithelial resistance measurement

Caco-2 cells (1 × 10<sup>5</sup> cells) were seeded on the apical compartment of transwell filters with 0.4 µm pore size (Corning Incorporated, USA). 0.5 mL and 1.5 mL of culture medium were added to the apical and basolateral compartment, respectively. 21 days after Caco-2 cells confluent, experiments were conducted. Before treatment, Caco-2 cells were transferred into serum-free DMEM containing 100 µg/mL gentamicin. Then, 20 µL EcN<sup>sup</sup> was added to the apical compartment of transwell in the presence or absence of 10 µM SN-38, which was applied to the basolateral sides. Transepithelial electrical resistance (TER) was measured with a Millicel-ERS-2 volt-ohmmeter (Millipore).

## 2.11. FD-4 flux measurement

Epithelial permeability was assessed as previously reported [31]. Briefly, following the treatment mentioned above, Caco-2 cells were washed with PBS and incubated in the upper compartment with Hank's balanced salt solution containing 1 mg/mL FD4 solution for 2 h. FD-4 flux was measured by taking 100 µL from the basolateral side. Fluorescent signal was assessed with Synergy H2 microplate reader (Biotek Instruments, USA) using 490 nm excitation and 520 nm emission filters.

## 2.12. Statistical analysis

The results were described as mean ± standard error of the mean (SEM) and analyzed using one-way ANOVA followed by Tukey's test. Statistical analysis was carried out using GraphPad Prism (version8.0; GraphPad Software, San Diego, CA, USA). *P* value < 0.05 was regarded as statistically significant.

## 3. Results

### 3.1. EcN reduced weight loss and diarrhea in irinotecan-treated mice

As shown in Fig. 1A, compared to control and irinotecan groups, mice pre-treated with EcN in the first 9 days did not suffer weight loss. However, irinotecan significantly induced weight loss compared with control group, and EcN administration attenuated the weight loss at Day 14. In addition, diarrhea was first observed 4 days after the first dose of irinotecan injection in irinotecan-treated mice. While co-treatment with EcN remarkably attenuated the diarrhea severity compared to irinotecan group (Fig. 1B). Interestingly, heat treatment abolished the effect of viable EcN on weight loss and diarrhea.

### 3.2. EcN protected mice against irinotecan-induced intestinal barrier dysfunction

Increased intestinal permeability, indicator of intestinal barrier dysfunction, is commonplace during chemotherapy [9]. The FD-4 concentration in plasma was significantly increased in irinotecan-treated mice compared to control group. EcN administration, but not heat-inactivated EcN, remarkably attenuated the increased FD-4 concentration induced by irinotecan (Fig. 1C). In summary, the findings indicated that only viable EcN prevented irinotecan-induced intestinal barrier dysfunction in mice. Thus, only viable EcN was used in the following experiment.

### 3.3. EcN alleviated intestinal mucosal damage induced by irinotecan

The histopathological and morphological analyses of distal ileum were performed by HE staining (Fig. 1D). The intestinal mucosa from control group showed intact morphology characteristic by finger-like elongated structures and compactly arrayed epithelium. However, the

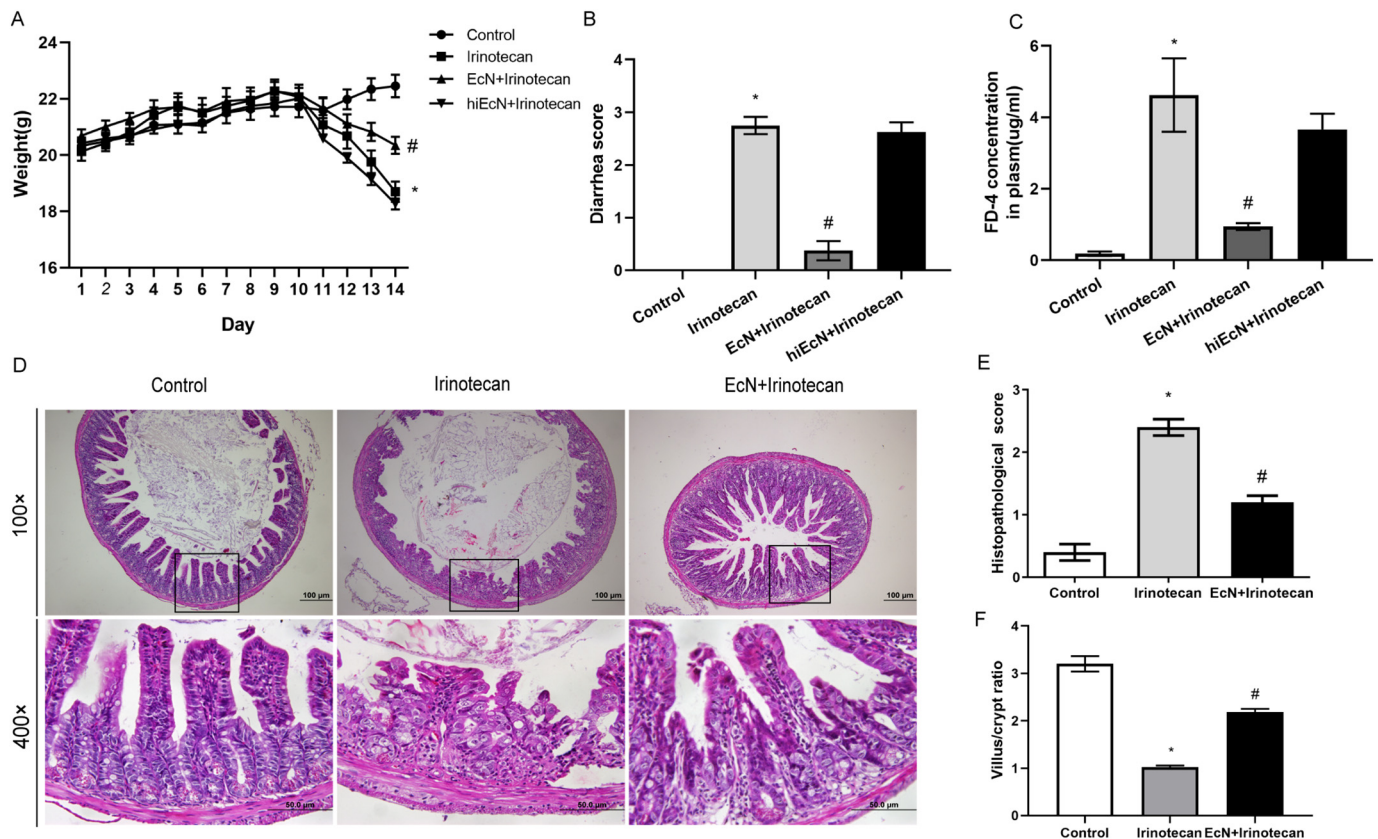


**Fig. 1.** Effect of EcN on the clinical and histopathological evaluations, barrier function of mice receiving irinotecan treatment. (A) Body weight. EcN significantly attenuated the weight loss in irinotecan-treated mice. (B) Diarrhea score at Day 14. EcN administration significantly alleviated the diarrhea severity induced by irinotecan. (C) FD-4 concentration. EcN remarkably inhibited the increased FD-4 concentration in plasma induced by irinotecan. (D) H&E staining. EcN administration attenuated the mucosal damage caused by irinotecan. (E) Histopathological score. EcN significantly suppressed the increased histopathological score in mice treated with irinotecan. (F) Villus/crypt ratio. EcN significantly ameliorated the irinotecan-induced reduction of villus/crypt ratio. The scale bar represents 100  $\mu$ m (magnification 100 $\times$ ) or 50  $\mu$ m (magnification 400 $\times$ ). hiEcN + Irinotecan: heat-inactivated EcN + irinotecan group. Values are represented as means  $\pm$  SEM. \* $P < 0.05$  vs Control. # $P < 0.05$  vs Irinotecan.

intestinal mucosa from irinotecan group represented severe intestinal damage featured by villus stunting, crypt disruption, inflammatory cells infiltration, the loss of crypt architecture, disorder of the epithelial cell layer, resulting in a high histopathological score (Fig. 1E). These histopathological abnormalities were restored by EcN administration. In addition, villus height and crypt depth ratio was measured. As shown in Fig. 1F, the villus/crypt ratio in mice treated with irinotecan was significantly decreased compared with the control group, while co-treatment with EcN significantly restored the decreased villus/crypt ratio.

Taken together, these results indicated that EcN pretreatment protected mice from irinotecan-induced intestinal mucosal damage.

### 3.4. EcN inhibited the irinotecan-induced decreased Claudin-1 expression

The expression of tight junction protein ZO-1, Occludin and Claudin-1 was measured by western blot. As shown in Fig. 2A, the expression of Claudin-1 was significantly decreased in irinotecan-treated mice compared with control group. However, ZO-1 and Occludin expression was not modified by irinotecan. Interestingly, EcN significantly restored the decreased Claudin-1 expression.

Consistently, immunofluorescence of tight junctions in distal ileum demonstrated that irinotecan significantly induced decreased staining intensity of Claudin-1, while the staining intensity of ZO-1 and Occludin was not changed by irinotecan treatment (Fig. 2C–E). EcN administration ameliorated the change of Claudin-1 induced by irinotecan.

To sum up, these results suggested that EcN attenuated the

irinotecan-induced intestinal barrier dysfunction partly through preserving Claudin-1 expression.

### 3.5. EcN modulated gut microbiota in irinotecan-treated mice

16S rRNA sequencing was performed to evaluate the modification in the intestinal microbiota composition among different treatment groups. Observed species, chao and ace indices reflect species richness of community (Fig. 3A–C). Irinotecan significantly decreased the richness of microbiota in cecum contents compared to control group. Shannon index which represents gut microbiota diversity was significantly decreased in irinotecan-treated mice compared to control group (Fig. 3D). However, EcN administration was able to restore all these indices to normal values. PCA and principal coordinates analysis (PCoA) based on the weighted and unweighted UniFrac distance matrices showed distinct separation of two treatment groups, which indicated that the community structure of the microbiota in irinotecan treated mice significantly differed from those in control group, and the overall structure of gut microbiota in mice pretreated with EcN also clearly distinct from those in irinotecan group (Fig. 3E–G). The system clustering tree based on Bray-Curtis distance also demonstrated significant differences among groups (Fig. 3H). The distance between EcN + irinotecan group and control group was smaller, which indicated a higher similarity in the microbiota communities between the two groups.

We further analyzed the difference in the relative abundance of gut microbiota species among different groups. Bacteroidetes and

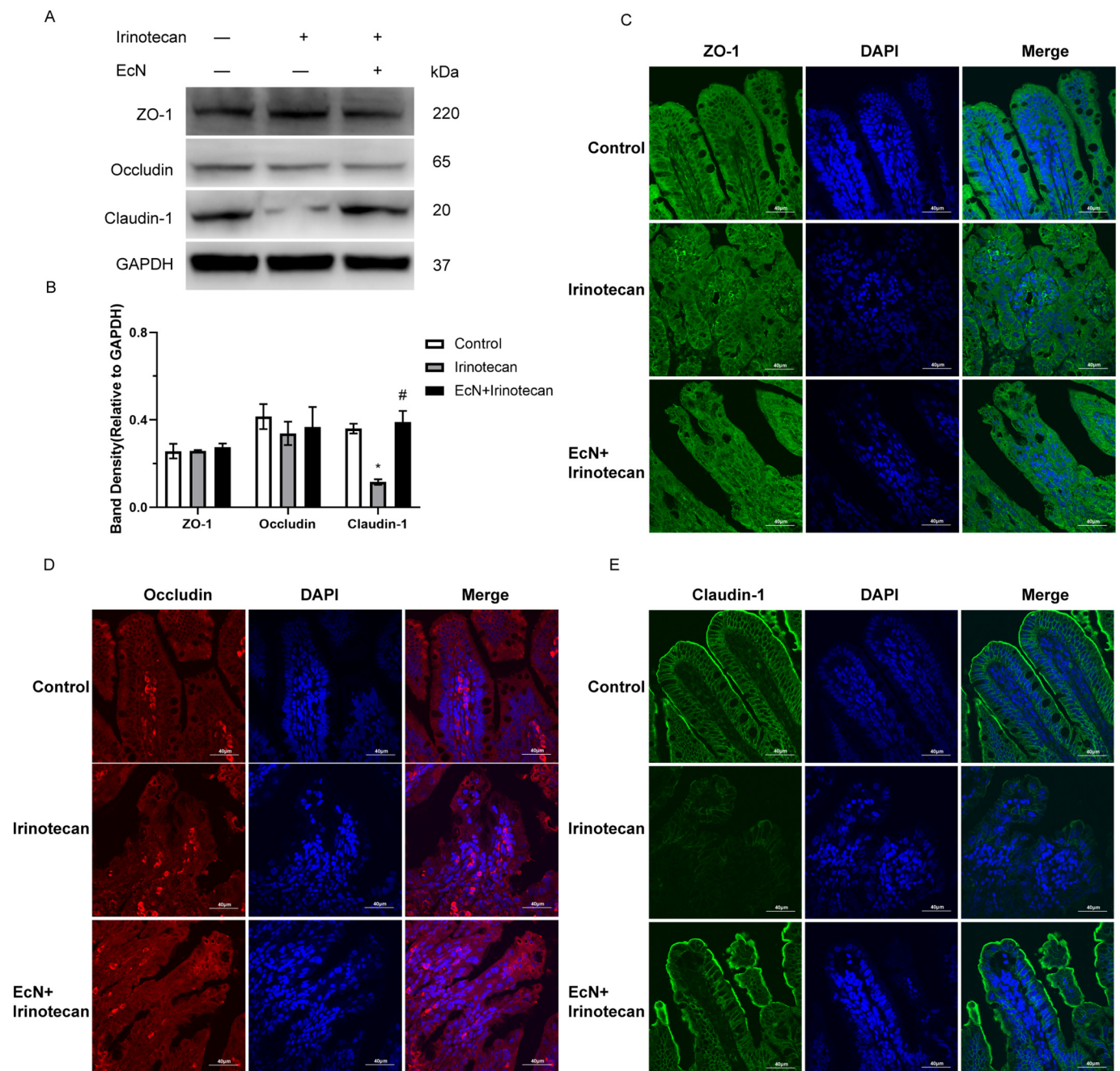


**Fig. 2.** Effect of EcN on the expression of tight junction proteins in irinotecan-treated mice. (A–B) Western blot of tight junctions. EcN administration inhibited the decreased expression of Claudin-1 in irinotecan-treated mice. The expression of ZO-1 and Occludin was not changed in the present study. (C–E) Immunofluorescence of tight junctions. Representative immunofluorescence images of ZO-1 (C, green), Occludin (D, red), Claudin-1 (E, green) in distal ileum. EcN ameliorated the irinotecan-induced reduction of Claudin-1 staining intensity. While the staining intensity of ZO-1 and Occludin was not affected by irinotecan or EcN treatment. Values are represented as means  $\pm$  SEM. \* $P < 0.05$  vs Control. # $P < 0.05$  vs Irinotecan. (For interpretation of the references to color in this figure legend, the reader is referred to the web version of this article.)

Firmicutes were the predominant phyla in gut microbiota of all groups (Fig. 4A–B). However, no significant differences in the relative abundance of Bacteroidetes and Firmicutes were observed among different treatment groups. In addition, the relative abundance of Proteobacteria phylum was remarkably increased in irinotecan-treated mice compared to control group, while EcN administration was able to ameliorate the increased level of Proteobacteria. Further analysis at class level revealed that irinotecan treatment significantly increased the relative abundance of Porphyromonadaceae and Mogibacteriaceae compared to control group, while EcN administration could reverse the changes. Moreover, a significant decreased in the relative abundance of

Rikenellaceae in irinotecan-treated mice was observed, which was reversed by EcN administration (Fig. 4C–D).

### 3.6. EcN<sup>sup</sup> prevented the SN-38-induced epithelial barrier dysfunction in Caco-2 cell monolayers

EcN<sup>sup</sup> and SN-38 were adopted in the current study. SN-38 is the active metabolite of irinotecan. To investigate the effects of EcN<sup>sup</sup> and SN-38 on intestinal epithelial barrier function, Caco-2 cell monolayers were treated with 10  $\mu$ M SN-38 and 20  $\mu$ L EcN<sup>sup</sup>. TER and FD-4 flux were used to assess Caco-2 monolayer barrier function. After 2 days of

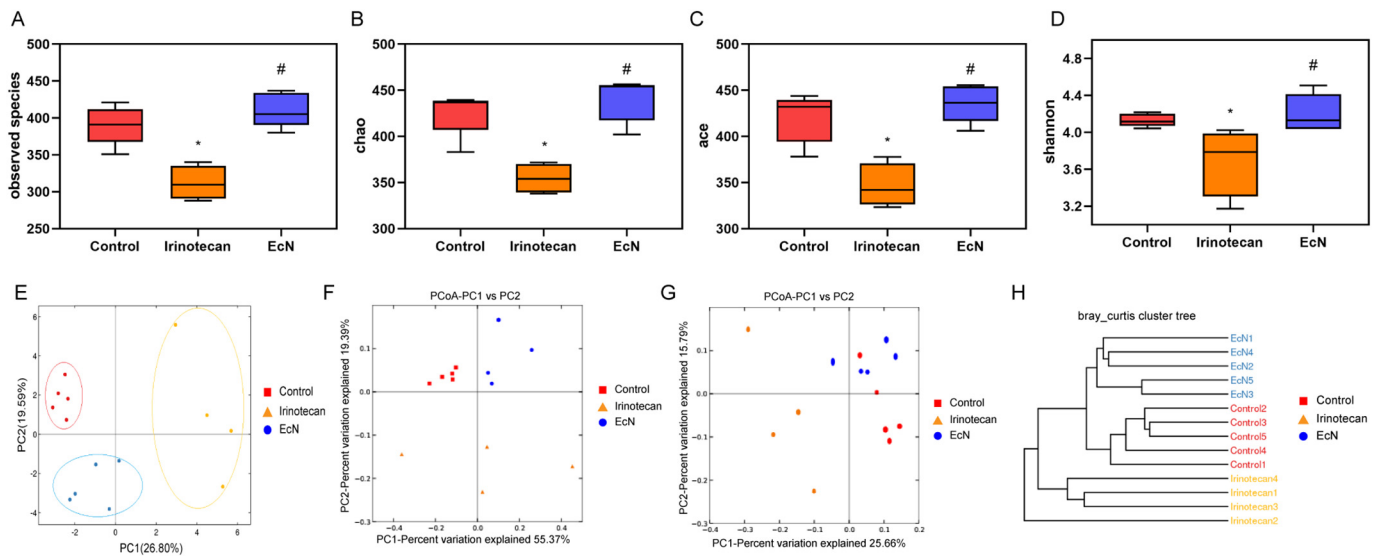


**Fig. 3.** Effect of EcN on the disturbed gut microbiota in irinotecan-treated mice. (A–C) Observed species, chao and ace indices are indicators of the community richness. EcN restored the decreased richness of gut microbiota in irinotecan-treated mice. (D) Shannon index is an estimator of community diversity. EcN prevented the decreased richness of gut microbiota in irinotecan-treated mice. PCA analysis (E), principal coordinates analysis (PCoA) based on the weighted (F) and unweighted (G) UniFrac distance matrices, system clustering tree based on Bray–Curtis distance (H) indicated the community structure of gut microbiota differed among groups. Control: control group ( $n = 5$ ), Irinotecan: irinotecan group ( $n = 4$ ), EcN: EcN + irinotecan group ( $n = 5$ ). Values are represented as means  $\pm$  SEM. \* $P < 0.05$  vs Control. # $P < 0.05$  vs Irinotecan.

treatment, SN-38 significantly induced disruption of monolayer barrier function, characterized by reduced TER and increased FD-4 flux. Co-treatment with EcN<sup>sup</sup> significantly ameliorated the monolayer barrier function injury (Fig. 5A–B).

### 3.7. EcN<sup>sup</sup> attenuated the alteration of Claudin-1 induced by SN-38

To explore the underlying mechanism involved in the protective effect of EcN<sup>sup</sup> on Caco-2 monolayers treated with SN-38, the expression and distribution of tight junction proteins were assessed. As shown in Fig. 5C, the expression of ZO-1, Occludin, and Claudin-1 was not affected by SN-38 or EcN<sup>sup</sup> treatment. However, altered localization and distribution of Claudin-1, which was characteristic by irregular staining, was observed following SN-38 treatment, as presented by immunofluorescence of Caco-2 cells (Fig. 5E). Co-treatment with EcN<sup>sup</sup> restored the modification of Claudin-1 induced by SN-38.

## 4. Discussion

Chemotherapy-induced gut toxicity is intensively related to the alteration in intestinal barrier function and gut microbiota. Recent studies indicated that EcN improved intestinal barrier function and regulated the disturbed gut microbiota in DSS mice [19,21]. So we hypothesized that EcN might protect against the gut damage resulted from irinotecan. In the present study, we showed that EcN ameliorated irinotecan-induced tight junction disruption and gut microbiota dysbiosis. In addition, considering that viable probiotics may pose risk to immunocompromised patients, we also investigated the effect of heat-inactivated EcN. However, our results indicated that heat-inactivated EcN did not prevent irinotecan-induced intestinal barrier dysfunction. Thus, viable EcN is essential for the protective effect against irinotecan-induced intestinal injury in the current study.

Chemotherapeutic agents, which target rapidly dividing cells to treat cancer, also injure such cells of intestinal epithelium and contribute to various gastrointestinal symptoms. Among these side effects, diarrhea is of particular clinical importance [32]. Our results consisted with previous study indicated that irinotecan induced significant diarrhea and weight loss [22]. We further illustrated that EcN administration effectively ameliorated the diarrhea and weight loss caused by

irinotecan. Other studies also demonstrated that probiotics administration, such as VSL#3, significantly reduced weight loss and diarrhea severity induced by irinotecan [33]. EcN supernatant alleviated the weight loss in 5-FU treated rats [34]. Furthermore, histopathological analysis of the ileum confirmed the protective effect of EcN on preserving intestinal mucosa integrity. As demonstrated in other report, irinotecan treatment resulted in shortening of villi and disruption of crypts [35]. While supplementation with EcN pronouncedly preserved the architecture of intestinal mucosa in mice.

Intestinal barrier function plays a vital role in maintaining gut homeostasis. Tight junctions are mainly responsible for the restriction and modulation of intestinal permeability. Disruption of intestinal barrier function is characterized by increased intestinal permeability [36]. Numerous studies have intensively demonstrated the increased intestinal permeability and altered tight junction protein expression during chemotherapy [8,9]. Irinotecan significantly induced increased intestinal permeability in mice [37]. Further research indicated that irinotecan decreased ZO-1, Occludin and Claudin-1 expression in rats [35]. Other study also validated down-regulated Claudin-1 and Occludin in irinotecan-treated rats, but ZO-1 expression remained unchanged [9]. In the current study, we found that irinotecan significantly increased the intestinal permeability and decreased the expression of Claudin-1, while no significant decreased of ZO-1 and Occludin expression was observed in irinotecan-treated mice. Claudin-1 is a key tight junction protein which restrains ions entrance to the epithelium and interacts with other claudins, forming the barrier that avoids lipid and protein diffusion [38]. Previous report indicated that decreased Claudin-1 expression resulted in increased intestinal permeability in IBS patients [39]. While enhanced expression of Claudin-1 contributed to the restoration of normal intestinal permeability [40]. In addition, overexpression of Claudin-1 enhanced barrier function characteristic by increased TER and decreased FITC-dextran in MDCK cells [41]. One study performed on cdx2-IEC monolayer indicated that Claudin-1 was essential for epithelial barrier function. The knock-down of Claudin-1 impaired normal monolayer barrier, while overexpression of Claudin-1 enhanced epithelial tightness [42]. Besides, although no significant alteration of tight junction proteins expression was observed, irinotecan induced internalization of Claudin-1 and increased paracellular permeability in wild-type mice. While TLR4<sup>-/-</sup> mice maintained

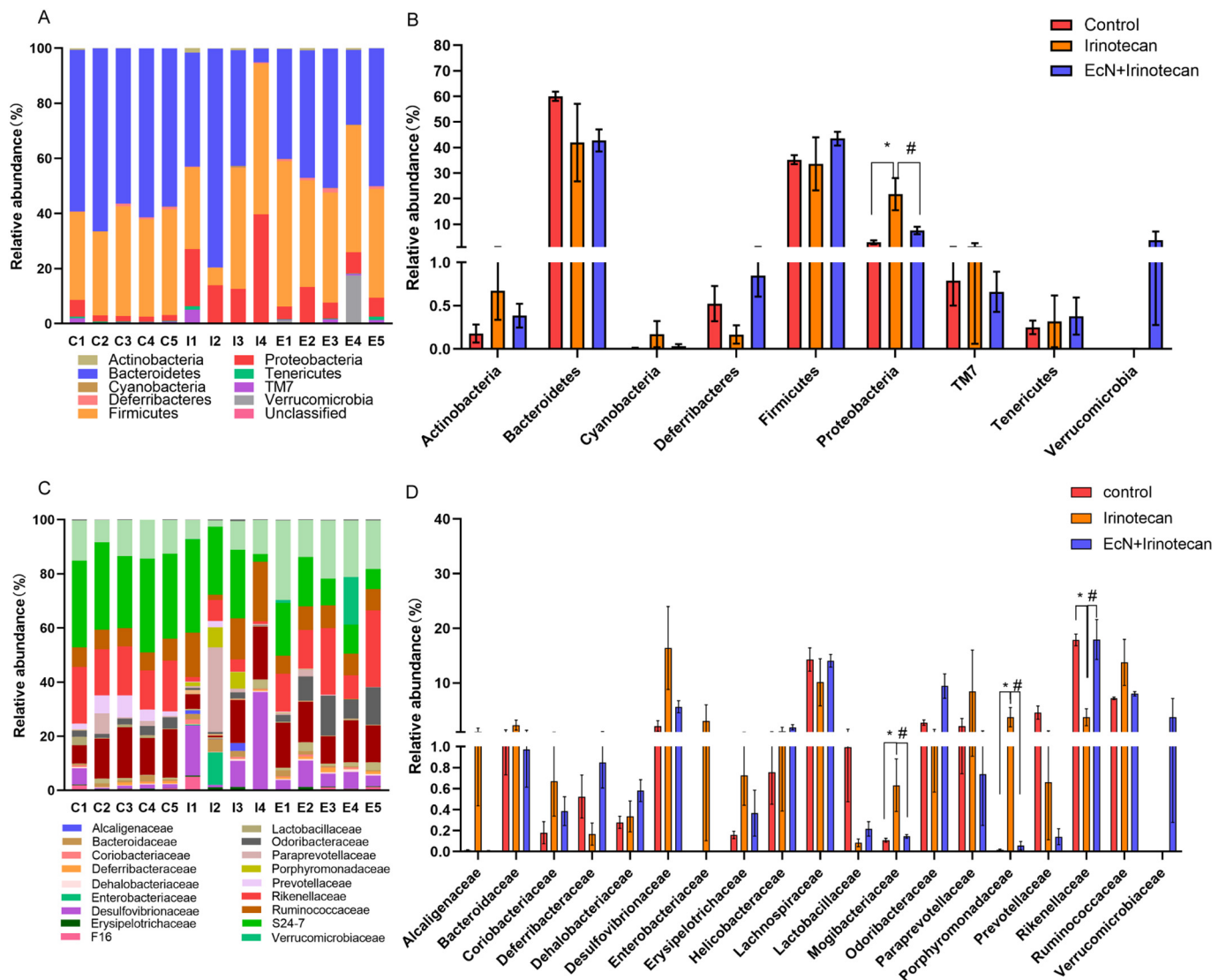


**Fig. 4.** Effect of EcN on the composition and relative abundance of microbiota in irinotecan-treated mice. (A–B) At phylum level. (C–D) At class level. Control group (n = 5), irinotecan group (n = 4), EcN + irinotecan group (n = 5). Values are represented as means  $\pm$  SEM. \**P* < 0.05 vs Control. #*P* < 0.05 vs Irinotecan.

phenotypically normal tight junctions and paracellular permeability. It emphasized the role of Claudin-1 in preventing intestinal barrier dysfunction caused by irinotecan [37]. Considering these previous studies, we may possibly relate the irinotecan induced intestinal barrier function injury to the decreased Claudin-1 expression in the present study.

Furthermore, we showed that EcN administration prevented the decrease of Claudin-1 expression and the increase of intestinal permeability in irinotecan-treated mice. Previous study sufficiently demonstrated that EcN improved intestinal epithelial barrier function through up-regulating the tight junction proteins ZO-1 [19], ZO-2 [20] and Claudin-14 [5]. However, it is worth mentioning that previous study did not show the ability of EcN to upregulate Claudin-1. Ukena et al. reported that EcN improved mucosal integrity in dextran sodium sulfate (DSS)-induced colitic mice by reducing intestinal permeability and up-regulating ZO-1 [19]. Regrettably, they did not analyze Claudin-1 protein expression. In vitro, EcN improved intestinal barrier function through upregulation of Claudin-14 in the human epithelial HT-29/B6 cells, while the Claudin-1 expression was not affected by EcN treatment. However, the experiment was performed under physiological condition, and it is likely that EcN acts differently in pathological or physiological states [5]. Here in our study, we demonstrated that EcN attenuated the down-regulation of Claudin-1 in irinotecan-treated mice.

In addition, experiments were performed in vitro utilizing Caco-2 monolayers to further investigate the effect of EcN and irinotecan on epithelial barrier function. SN-38 is the active metabolite of irinotecan and is supposed to contribute to the intestinal damage during chemotherapy [4]. The protective effect of EcNsup on epithelial barrier function has been fully elaborated previously. Incubation with EcNsup led to a time-dependent increased TER in HT-29/B6 monolayers [5]. EcNsup reduced cell death and increased TER in IEC-6 cells treated with 5-FU [43]. In the present study, we showed that EcNsup reversed the SN-38 induced decreased TER and increased paracellular permeability in Caco-2 cells. Besides, although no modification of tight junction proteins expression was observed, co-treatment with EcNsup ameliorated altered cellular localization and distribution of Claudin-1 caused by SN-38. These results indicated that EcNsup preserved the epithelial barrier function from injuries resulted from SN-38 by maintaining the function of Claudin-1 in Caco-2 cells. The inconformity in change of Claudin-1 protein expression induced by irinotecan between mice and Caco-2 cells may be possibly explained by contributions from different studied models.

Maintenance of balanced gut microbiota is essential for intestinal homeostasis and human health. Gut microbial dysbiosis, which refers to altered composition of the gut microbiota, is a common side effect of

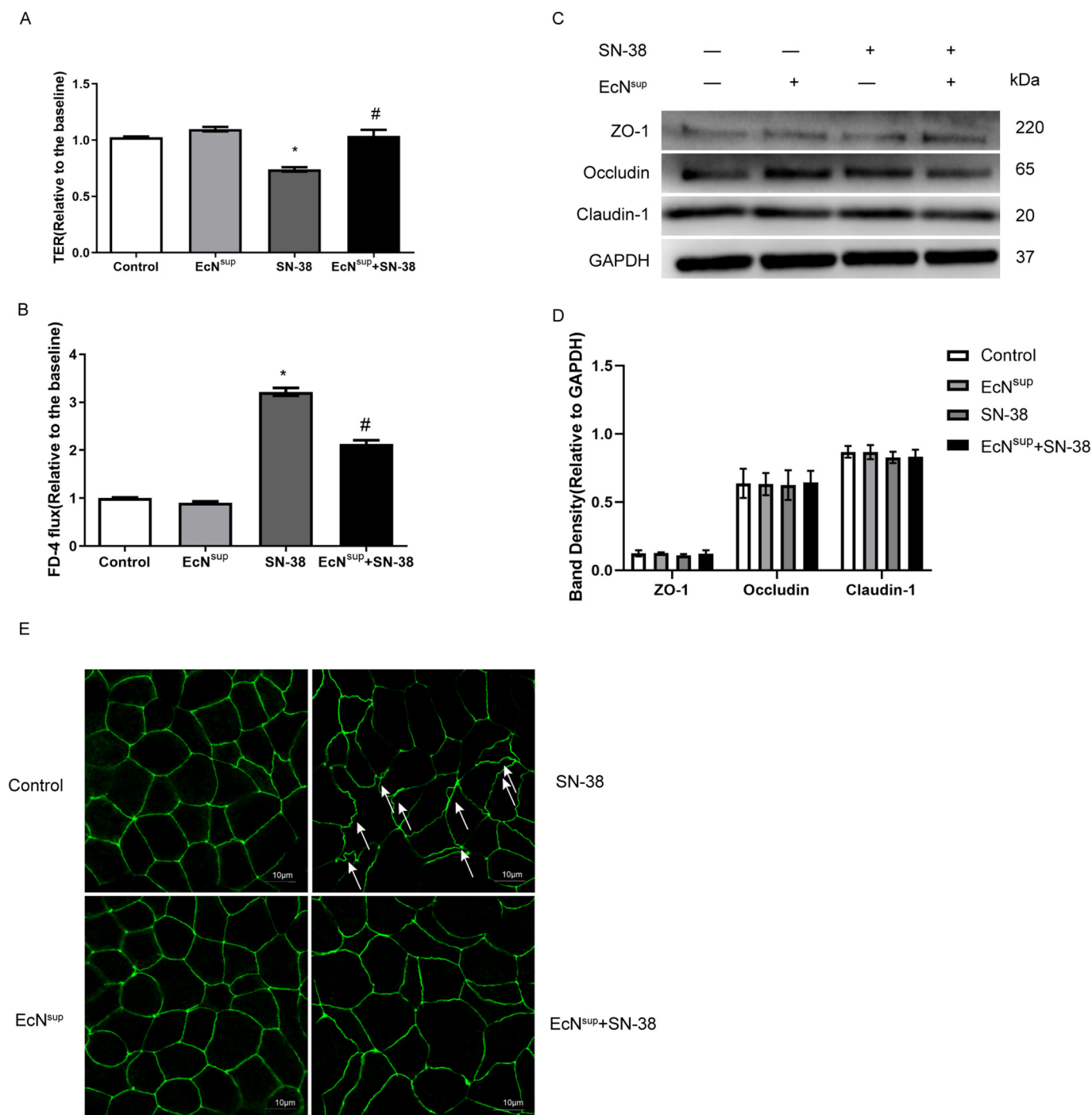


**Fig. 5.** Effect of EcN<sup>sup</sup> on the epithelial barrier function in Caco-2 monolayers treated with SN-38. (A) TER. (B) FD-4 flux. Caco-2 cell monolayers were treated with 20 μL EcN<sup>sup</sup> with or without 10 μM SN-38, the TER and FD-4 flux were measured 48 h after treatment. EcN<sup>sup</sup> markedly ameliorated the SN-38-induced decreased TER and increased FD-4 flux. (C–D) Western blot of tight junctions. The expression of tight junctions was not changed by SN-38 or EcN<sup>sup</sup>. (E) Immunofluorescence of Claudin-1. EcN<sup>sup</sup> attenuated the altered localization and distribution of Claudin-1 induced by SN-38, which was characteristic by irregular staining (arrows). Values are represented as means ± SEM. \*P < 0.05 vs Control. #P < 0.05 vs SN-38.

chemotherapy. For example, irinotecan increased the relative abundance of Enterobacteriaceae and Clostridium cluster XI in rats [44]. 5-Fu diminished Clostridium, Lactobacillus, Streptococcus, Enterococcus and increased Escherichia in rats [45]. In the current study, we showed that irinotecan treatment induced a significant decrease in microbial diversity, as represented by observed species, chao, ace and Shannon indices, which consisted with previous report [13]. Reduced diversity of gut microbiota is a well-described characteristic of intestinal dysbiosis, which associates with multiple gastrointestinal disorders and

inflammatory states [13,46]. In addition, we found a significant increase in the relative abundance of Proteobacteria in irinotecan-treated mice. Proteobacteria, a minor proportion of gut microbiota, whose abnormal expansion is usually considered as a signature of dysbiosis in gut microbiota [47]. The abundance of Proteobacteria has been reported to increase in patients with inflammatory bowel disease [48]. Consistently, previous study indicated that irinotecan induced expansion of Proteobacteria in rats [13]. Moreover, the abundances of Enterobacteriaceae and Escherichia spp. were increased in rats following

irinotecan treatment [49]. *E. coli*, Gram-negative bacteria, is a member of Enterobacteriaceae family, which belongs to Proteobacteria. *E. coli* was able to produce lipopolysaccharides, which induced the production of pro-inflammatory factors through Toll-like receptor-linked NF- $\kappa$ B signaling pathways. Desulfovibrionaceae, H<sub>2</sub>S-producing family of Proteobacteria, was related to intestinal barrier injury [50]. In the present study, the relative abundances of Desulfovibrionaceae and Enterobacteriaceae were also increased in irinotecan-treated mice, but the increases did not reach statistical significance. Besides, Rikenellaceae, a member of Bacteroidetes family, was remarkably decreased by irinotecan treatment, which was also consistent with previous studies demonstrated that the relative abundance of Rikenellaceae was decreased in colitis status [51].

It is reported that chemotherapy-induced gut microbiota dysbiosis through diminishing beneficial bacteria and increasing potential pathogenic bacteria [52]. Thus, probiotics supplement could be a practical way to attenuate the dysbiosis induced by chemotherapy. Several lines of studies have demonstrated the protective effect of probiotics against dysbiosis. The probiotic mixture DM#1 was able to restore the intestinal homeostasis of 5-FU-treated rats and effective in preserving *Lactobacillus* spp., *Clostridium* clusters III and XIVa [53]. *Lactobacillus reuteri* F-9-35 reversed the imbalance of Firmicutes and Bacteroidetes of gut microbiota in DDS mice [54]. Furthermore, *Escherichia coli* Nissle 1917 ameliorated the altered gut microbiome in DSS mice, especially reduced microbiota diversity [21]. Here, we showed that EcN administration improved the decreased diversity of intestinal microbiota and restored the altered microbial community in irinotecan-treated mice, especially the excessive abundance of Proteobacteria.

## 5. Conclusion

To our knowledge, this is the first study to analyze the protective effect of EcN against irinotecan-induced intestinal injury. Our data suggested that the prophylactic administration of EcN ameliorated irinotecan-induced intestinal barrier dysfunction and gut microbial dysbiosis. The protective effect of EcN against intestinal barrier dysfunction elicited by irinotecan might be mediated by the modulation of Claudin-1. Additionally, EcN restored the decreased diversity of gut microbiota and the increased abundance of Proteobacteria induced by irinotecan. Our findings provide preliminary evidence supporting the potential of EcN as a novel treatment strategy for irinotecan-induced intestinal injury. However, further investigations are warranted to focus on the underlying mechanism of EcN.

## Acknowledgments

This work is supported by the grant for the protective effect of hydrogen sulfide on the intestinal barrier and multiple organ dysfunction in septic shock and the underlying mechanisms from The National Natural Science Foundation of China (8177030343).

## Declaration of Competing Interest

The authors declare that there are no conflicts of interest.

## References

- [1] Y. Touchefeu, E. Montassier, K. Nieman, T. Gastinne, G. Potel, S. Varannes, Bruley Des, et al., Systematic review: the role of the gut microbiota in chemotherapy- or radiation-induced gastrointestinal mucositis - current evidence and potential clinical applications, *Aliment Pharmacol Ther.* 40 (2014) (n/a-n/a).
- [2] R.W. Bastos, S.H. Pedrosa, A.T. Vieira, L.M. Moreira, Franãsa CS, C.T. Cartelle, et al., *Saccharomyces cerevisiae* UFMG A-905 treatment reduces intestinal damage in a murine model of irinotecan-induced mucositis, *Benefic. Microbes* 7 (2016) 549–557.
- [3] L. Iyer, C.D. King, P.F. Whittington, M.D. Green, S.K. Roy, T.R. Tephly, et al., Genetic predisposition to the metabolism of irinotecan (CPT-11). Role of uridine diphosphate glucuronosyltransferase isoform 1A1 in the glucuronidation of its active metabolite (SN-38) in human liver microsomes, *J Clin Invest.* 101 (1998) 847.
- [4] R.A. Ribeiro, C.W.S. Wanderley, D.V.T. Wong, J.M.S.C. Mota, C.A.V.G. Leite, M.H.L.P. Souza, et al., Irinotecan- and 5-fluorouracil-induced intestinal mucositis: insights into pathogenesis and therapeutic perspectives, *Cancer Chemother. Pharmacol.* 78 (2016) 881–893.
- [5] N.A. Hering, J.F. Richter, A. Fromm, A. Wieser, S. Hartmann, D. Günzel, et al., Tcpc protein from *E. coli* Nissle improves epithelial barrier function involving PKC $\zeta$  and ERK1/2 signaling in HT-29/B6 cells, *Mucosal Immunol.* 7 (2014) 369–378.
- [6] H.R. Wardill, J.M. Bowen, Chemotherapy-induced mucosal barrier dysfunction: an updated review on the role of intestinal tight junctions, *Curr Opin Support Palliat Care* 7 (2013) 155–161.
- [7] T. Kucharzik, S.V. Walsh, J. Chen, C.A. Parkos, A. Nusrat, Neutrophil transmigration in inflammatory bowel disease is associated with differential expression of epithelial intercellular junction proteins, *Am. J. Pathol.* 159 (2001) 2001–2009.
- [8] Y.S. Beutheu, L. Belmonte, L. Galas, N. Boukhattala, C. Bôle-Feysoot, P. Déchelotte, et al., Methotrexate modulates tight junctions through NF- $\kappa$ B, MEK, and JNK pathways, *J. Pediatr. Gastroenterol. Nutr.* 54 (2012) 463–470.
- [9] N. Toshihiro, K. Nobuhiro, K. Masato, Y. Kozo, I. Takashi, U. Toru, et al., Irinotecan injures tight junction and causes bacterial translocation in rat, *J. Surg. Res.* 173 (2012) 341–347.
- [10] A. Sircana, L. Framarin, N. Leone, M. Berrutti, F. Castellino, R. Parente, et al., Altered gut microbiota in type 2 diabetes: just a coincidence? *Current Diabetes Reports* 18 (2018) 98.
- [11] M. Tong, X. Li, L. Wegener Parfrey, B. Roth, A. Ippoliti, B. Wei, et al., A modular organization of the human intestinal mucosal microbiota and its association with inflammatory bowel disease, *PLoS One* 8 (2013) e80702.
- [12] G. Musso, R. Gambino, M. Cassader, Interactions between gut microbiota and host metabolism predisposing to obesity and diabetes, *Annu. Rev. Med.* 62 (2012) 361–380.
- [13] R.A. Forsgård, V.G. Marrachelli, K. Korpela, R. Frias, M.C. Collado, R. Korpela, et al., Chemotherapy-induced gastrointestinal toxicity is associated with changes in serum and urine metabolome and fecal microbiota in male Sprague–Dawley rats, *Cancer Chemother. Pharmacol.* 80 (2017) 317–332.
- [14] C.H. Wu, J.L. Ko, J.M. Liao, S.S. Huang, M.Y. Lin, L.H. Lee, et al., D-methionine alleviates cisplatin-induced mucositis by restoring the gut microbiota structure and improving intestinal inflammation, *Ther Adv Med Oncol* 11 (2019) 1758835918821021.
- [15] G.A. Preidis, V. James, Targeting the human microbiome with antibiotics, probiotics, and prebiotics: gastroenterology enters the metagenomics era, *Gastroenterology.* 136 (2009) 2015–2031.
- [16] R. Chibbar, L.A. Dieleman, Probiotics in the management of ulcerative colitis, *J. Clin. Gastroenterol.* 49 (Suppl. 1) (2015) S50.
- [17] D. Katarzyna, H.M. Magdalena, S. Marcin, S. Jakub, B. Tomasz, Probiotics in the mechanism of protection against gut inflammation and therapy of gastrointestinal disorders, *Curr. Pharm. Des.* 20 (2014).
- [18] S. Miriam, W. Jan, A. Artur, T.A. Oelschlaeger, E.F. Stange, F. Klaus, Induction of human beta-defensin 2 by the probiotic *Escherichia coli* Nissle 1917 is mediated through flagellin, *Infect. Immun.* 75 (2007) 2399–2407.
- [19] S.N. Ukena, S. Anurag, D. Ulrike, E. Regina, S. Ursula, H. Wiebke, et al., Probiotic *Escherichia coli* Nissle 1917 inhibits leaky gut by enhancing mucosal integrity, *PLoS One* 2 (2007) e1308.
- [20] A.A. Zyrek, C. Cichon, S. Helms, C. Enders, U. Sonnenborn, M.A. Schmidt, Molecular mechanisms underlying the probiotic effects of *Escherichia coli* Nissle 1917 involve ZO-2 and PKC $\zeta$  redistribution resulting in tight junction and epithelial barrier repair, *Cell. Microbiol.* 9 (2007) 804–816.
- [21] A. Rodrigueznogales, F. Algieri, J. Garridomesa, T. Vezza, M.P. Utrilla, N. Chueca, et al., The administration of *Escherichia coli* Nissle 1917 ameliorates development of DSS-induced colitis in mice, *Front. Pharmacol.* 9 (2018) 468.
- [22] Q. Lian, J. Xu, S. Yan, M. Huang, H. Ding, X. Sun, et al., Chemotherapy-induced intestinal inflammatory responses are mediated by exosome secretion of double-strand DNA via AIM2 inflammasome activation, *Cell Res.* 27 (2017) 784.
- [23] L.C. Tong, Y. Wang, Z.B. Wang, W.Y. Liu, S. Sun, L. Li, et al., Propionate ameliorates dextran sodium sulfate-induced colitis by improving intestinal barrier function and reducing inflammation and oxidative stress, *Front. Pharmacol.* 7 (2016).
- [24] R.C.P. Lima-Júnior, A.A. Figueiredo, H.C. Freitas, M.L.P. Melo, D.V.T. Wong, C.A.V.G. Leite, et al., Involvement of nitric oxide on the pathogenesis of irinotecan-induced intestinal mucositis: role of cytokines on inducible nitric oxide synthase activation, *Cancer Chemother. Pharmacol.* 69 (2012) 931–942.
- [25] B.R. Macpherson, C.J. Pfeiffer, Experimental production of diffuse colitis in rats, *Digestion.* 17 (1978) 135–150.
- [26] P.W. Lin, L.E.S. Myers, R. Laurie, S. Shuh-Chyung, T.R. Nasr, A.J. Berardinelli, et al., *Lactobacillus rhamnosus* blocks inflammatory signaling in vivo via reactive oxygen species generation, *Free Radic. Biol. Med.* 47 (2009) 1205–1211.
- [27] K. Juan, Z. Zhongyi, M.W. Musch, N. Gang, S. Jun, H. John, et al., Novel role of the vitamin D receptor in maintaining the integrity of the intestinal mucosal barrier, *Am. J. Physiol. Gastrointest. Liver Physiol.* 294 (2008) 208–216.
- [28] H.C. Chou, C.M. Chen, Neonatal hyperoxia disrupts the intestinal barrier and impairs intestinal function in rats, *Exp. Mol. Pathol.* 102 (2017) 415.
- [29] S.W. Chen, Y.Y. Ma, J. Zhu, S. Zuo, J.L. Zhang, Z.Y. Chen, et al., Protective effect of 1,25-dihydroxyvitamin D 3 on ethanol-induced intestinal barrier injury both in vitro and in vivo, *Toxicol. Lett.* 237 (2015) 79–88.
- [30] E. Gülden, C. Chao, N. Tai, J.A. Pearson, J. Peng, M. Majewska-Szczepanik, et al., TRIF deficiency protects non-obese diabetic mice from type 1 diabetes by modulating the gut microbiota and dendritic cells, *Journal of Autoimmunity* 93 (2018) 57–65 (S0896844118302580).
- [31] Q. Muhammad, R. Hazir, A. Raees, O. Michael, A.R. Asif, Mycophenolic acid

- mediated disruption of the intestinal epithelial tight junctions, *Exp. Cell Res.* 322 (2014) 277–289.
- [32] A. Jervoise, R. Paul, D. Clare, L. Elaine, L. Pauline, W. Caroline, et al., Guidance on the management of diarrhoea during cancer chemotherapy, *Lancet Oncol.* 15 (2014) (e447–e60).
- [33] J.M. Bowen, A.M. Stringer, R.J. Gibson, A.S. Yeoh, S. Hannam, D.M. Keefe, VSL#3 probiotic treatment reduces chemotherapy-induced diarrhea and weight loss, *Cancer Biology & Therapy* 6 (2007) 1445–1450.
- [34] H. Wang, Y.D. Jatmiko, S.E.P. Bastian, S. Mashtoub, G.S. Howarth, Effects of supernatants from *Escherichia coli* Nissle 1917 and *Faecalibacterium prausnitzii* on intestinal epithelial cells and a rat model of 5-fluorouracil-induced mucositis, *Nutr. Cancer* 69 (2017) 307–318.
- [35] H.R. Wardill, J.M. Bowen, N. Al-Dasooqi, M. Sultani, E. Bateman, R. Stansborough, et al., Irinotecan disrupts tight junction proteins within the gut: implications for chemotherapy-induced gut toxicity, *Cancer Biology & Therapy.* 15 (2014) 236–244.
- [36] S.H. Lee, Intestinal permeability regulation by tight junction: implication on inflammatory bowel diseases, *Intestinal Research* 13 (2015) 11.
- [37] H.R. Wardill, J.M. Bowen, Y.Z. Van Sebille, K.R. Secombe, J.K. Collier, I.A. Ball, et al., TLR4-dependent claudin-1 internalization and secretagogue-mediated chloride secretion regulate irinotecan-induced diarrhea, *Mol. Cancer Ther.* 15 (2016) 2767.
- [38] P. Cuellar, E. Hernández-Nava, G. García-Rivera, B. Chávez-Munguía, M. Schnoor, A. Betanzos, et al., *Entamoeba histolytica* EhCP112 dislocates and degrades Claudin-1 and Claudin-2 at tight junctions of the intestinal epithelium, *Front. Cell. Infect. Microbiol.* 7 (2017) 372.
- [39] B.V.L. Nathalie, Y. Stéphanie Beutheu, B. Liliana, L. Stéphane, A. Michel, G. Guillaume, et al., The expression and the cellular distribution of the tight junction proteins are altered in irritable bowel syndrome patients with differences according to the disease subtype, *Am. J. Gastroenterol.* 106 (2011) 2165–2173.
- [40] Z. Qiqi, C. Stefan, C.M. Croce, A.R. Brasier, M. Shehzad, S.A. Larson, et al., MicroRNA 29 targets nuclear factor- $\kappa$ B-repressing factor and Claudin 1 to increase intestinal permeability, *Gastroenterology* 148 (2015) (158–69.e8).
- [41] T. Inai, J. Kobayashi, Y. Shibata, Claudin-1 contributes to the epithelial barrier function in MDCK cells, *Eur. J. Cell Biol.* 78 (1999) 849.
- [42] H.B. Wang, P.Y. Wang, W. Xin, Y.L. Wan, Y.C. Liu, Butyrate enhances intestinal epithelial barrier function via up-regulation of tight junction protein Claudin-1 transcription, *Dig. Dis. Sci.* 57 (2012) 3126–3135.
- [43] W. Hanru, S.E.P. Bastian, K.Y. Cheah, L. Andrew, G.S. Howarth, *Escherichia coli* Nissle 1917-derived factors reduce cell death and late apoptosis and increase transepithelial electrical resistance in a model of 5-fluorouracil-induced intestinal epithelial cell damage, *Cancer Biology & Therapy.* 15 (2014) 560–569.
- [44] X.B. Lin, L.A. Dieleman, A. Ketabi, I. Bibova, M.B. Sawyer, H. Xue, et al., Irinotecan (CPT-11) chemotherapy alters intestinal microbiota in tumour bearing rats, *PLoS One* 7 (2012) e39764.
- [45] A.M. Stringer, R.J. Gibson, R.M. Logan, J.M. Bowen, A.S. Yeoh, J. Hamilton, et al., Gastrointestinal microflora and mucins may play a critical role in the development of 5-fluorouracil-induced gastrointestinal mucositis, *Exp. Biol. Med.* 234 (2009) 430.
- [46] M.J. Claesson, I.B. Jeffery, S. Conde, S.E. Power, E.M. O'Connor, S. Cusack, et al., Gut microbiota composition correlates with diet and health in the elderly, *Nature.* 488 (2012) 178–184.
- [47] N.R. Shin, T.W. Whon, J.W. Bae, Proteobacteria: microbial signature of dysbiosis in gut microbiota, *Trends Biotechnol.* 33 (2015) S0167779915001390.
- [48] I. Mukhopadhyay, R. Hansen, E.M. El-Omar, G.L. Hold, IBD-what role do Proteobacteria play? *Nat. Rev. Gastroenterol. Hepatol.* 9 (2012) 219–230.
- [49] A.M. Stringer, R.J. Gibson, R.M. Logan, J.M. Bowen, A.S. Yeoh, J. Burns, et al., Chemotherapy-induced diarrhea is associated with changes in the luminal environment in the DA rat, *Exp. Biol. Med.* 232 (2007) 96–106.
- [50] Y.Y. Lam, C.W. Ha, J.M. Hoffmann, J. Oscarsson, A. Dinudom, T.J. Mather, et al., Effects of dietary fat profile on gut permeability and microbiota and their relationships with metabolic changes in mice, *Obesity.* 23 (2015) 1429–1439.
- [51] M. Wu, Y. Wu, B. Deng, J. Li, H. Cao, Y. Qu, et al., Isoliquiritigenin decreases the incidence of colitis-associated colorectal cancer by modulating the intestinal microbiota, *Oncotarget.* 7 (2016) 85318–85331.
- [52] E. Montassier, T. Gastinne, P. Vangay, G.A. Al-Ghalith, dVS Bruley, S. Massart, et al., Chemotherapy-driven dysbiosis in the intestinal microbiome, *Aliment. Pharmacol. Ther.* 42 (2015) 515–528.
- [53] Y. Tang, Y. Wu, Z. Huang, W. Dong, Y. Deng, F. Wang, et al., Administration of probiotic mixture DM#1 ameliorated 5-fluorouracil-induced intestinal mucositis and dysbiosis in rats, *Nutrition.* 33 (2016) 96–104.
- [54] M.C. Sun, F.C. Zhang, X. Yin, B.J. Cheng, C.H. Zhao, Y.L. Wang, et al., *Lactobacillus reuteri* F-9-35 prevents DSS-induced colitis by inhibiting proinflammatory gene expression and restoring the gut microbiota in mice, *Journal of Food Science* 83 (2018) 2645–2652.